Probabilistic Cost Functions for Network Flow Phase Unwrapping

G.F. CARBALLO

Centro de Cálculo, Fac. Ingeniería

Montevideo, 11300, Uruguay

P.W. FIEGUTH

University of Waterloo

Waterloo, Ont., N2L-3G1, Canada

gabriel@fing.edu.uy Tel: (598-2)711-4229 Fax: (598-2)711-5446

Abstract

The well-studied Interferometric Synthetic Aperture Radar (InSAR) problem for digital elevation map generation involves the derivation of topography from radar phase. The topography is a function of the *full* phase, whereas the *measured* phase is known modulo 2π, necessitating the process of recovering full phase values via phase unwrapping. This mathematical process becomes difficult through the presence of noise and phase discontinuities. Our research is motivated by recent research which models phase unwrapping as a network flow minimization problem. The cost function to be optimized is a weighted L^1-norm of the phase discontinuities. Determining these cost weights is critical, yet past work in the literature does not reflect the statistics of the unwrapping problem.

The purpose of this paper is to propose a new method to compute the flow weights from a theoretical foundation. Specifically, we formulate phase-unwrapping as a Maximum Likelihood estimation problem, which we mathematically rewrite as a network flow problem with a specific choice of weights. The approach is based on estimating the probability of phase discontinuities, which can be derived as a function of coherence and topographic slope from the known statistical properties of SAR phase.

[0]Research supported in part by the Natural Sciences and Engineering Research Council of Canada, CCRS / GlobeSAR 2 and CONICYT-BID, Uruguay

1 Introduction

Synthetic Aperture Radar (SAR) interferometry[12, 19, 25] is an enormously promising technique in the generation of highly accurate elevation maps. The interest in such digital terrain maps stems from the vast number of disciplines which have a need for such basic data, namely hydrologic modeling, erosion studies, mining prospection, wildlife habitat, and military tactics, to name a few.

The basic premise of SAR interferometry is that by counting the phase fringes in an interference pattern, extremely sensitive measurements of elevation can be accomplished. In idealized settings, in which the phase measurements are noise-free, this approach is relatively straightforward (with the exception of steep topography). However actual measurements, taken from repeat-pass spaceborne SAR instruments such as Radarsat[11] or ERS[19], pose additional challenges in the form of decorrelation noise and atmospheric distortions. Since the measured phase values are known only modulo 2π, the absolute phase (which is related to the surface elevation) needs to be inferred by fringe-counting or phase-unwrapping[6, 14, 16, 20].

The most straightforward approach to phase unwrapping is to integrate the phase gradients. If all of the true phase gradients are bounded by one-half cycle (i.e., they lie in $[-\pi, \pi)$), then the integral along *any* path will yield the same result; this implies that the gradient integral around any simple closed loop is zero. However normally some pixels violate this hypothesis. That is, given that the original phase information is known only modulo 2π, a true gradient larger than one-half cycle (e.g., a discontinuity) will be wrapped to a different value, causing some closed-loop integrals to be non-zero (the so-called residues or charges) and the integrated phase between two pixels to be path-dependent, forcing the phase unwrapping algorithm to determine which path integrals it will believe. The task of a phase unwrapping algorithm is to add multiples of 2π to the phase-gradient between pixels to restore the condition that all closed-loop integrals be zero.

One current and widely-popular method for unwrapping is the minimum cost flow algorithm[4, 5, 6, 8, 21]. This approach uses network flow theory to convert the phase unwrapping problem to a discrete optimization problem, minimizing some total "cost" with the constraint that all loop integrals are zero. The conversion maps closed-loop integrals and pixel pairs into network nodes and arcs respectively, where the flow on each particular arc represents the residual (the number of 2π multiples in the preceding paragraph). Clearly the choice of the cost function is critical to finding an accurate solution, yet this issue has had little study.

Moreover, Chen & Zebker [4] recently showed that any unwrapped phase field can be completely specified by some flow meeting the network constraints. Hence, the different unwrapping algorithms share an essentially common goal: finding the feasible flow with the smallest total cost, where differences in algorithm objectives are reflected by differences in arc cost functions. Therefore, it would imply that the appropriate choice of the cost function acquires even more importance, since the costs are essentially the only parameters distinguishing between a large family of algorithms.

Many methods with varied costs have been proposed [6, 8, 21], however they have been ad-hoc, thresholding the SAR signal coherence[6] or applying edge-detection to the SAR amplitude[4]. The purpose of this paper is to propose a more systematic method for network-flow cost selection.

Figure 1 illustrates the kind of undesired effects that can arise when dealing with a constant cost function. We have a synthetic surface of two ramps, continuous except along a horseshoe arc. The coherence (a measure of the quality of the phase measurement) is qualitatively consistent with real data sets: the coherence is generally high, tapering to a low value (0.4) near surface discontinuities. The synthetic interferogram in Figure 1(c) clearly shows the phase fringes, with the fringe separation proportional to the surface slope. If we apply network-flow to the interferogram, the resulting surface differs from the original in that the centre ramp fails to be properly attached to the rest of the surface, as shown in Figure 6(a); this problem

of having discontinuities or "cuts" running across high-coherence areas has already been shown by other authors[8, 13].

In this paper we undertake the first systematic investigation of network flow costs. Our basic premise is the following: the cost of a pixel pair must reflect the "cost" of having an aliased phase (i.e. a non-zero residual), which must therefore clearly be a function of the probability that the pixel phase difference is aliased, or lying outside of $[-\pi, \pi)$. Therefore, we assert that at least two quantities need to be accounted in *any* sensible definition of costs — the coherence, which measures the signal-to-noise ratio of the phase, and the surface gradient, which influences the phase gradient and therefore the probability that a measured phase will be aliased. We develop such a cost model, dependent on both slope and coherence, based on an analogy with solving a Maximum Likelihood estimation problem. Moreover, this framework naturally leads to an asymmetric costs allocation, that is, it assigns different weights to positive and negative residuals.

Section 2 reviews network flow and clarifies the importance of costs. Sections 3 and 4 respectively derive the gradient aliasing probabilities and the network-flow costs. Section 5 compares our derived cost function with competing methods, and conclusions are summarized in Section 6.

2 Network Flow Algorithm

The purpose of this section is to introduce the reader to the network flow algorithm[5, 6, 8]. We are interested in the mathematical properties of the problem, rather than the specific details of a particular implementation. Since the main focus of our paper is to understand the behavior of the unwrapped solutions as a function of different costs, to avoid distraction we will treat the network-flow algorithm strictly as a tool or black-box.

As mentioned in the Introduction, the objective of a phase unwrapping algorithm is to locate discontinu-

ities. Most algorithms do so by means of minimizing the value of some objective function. Least-squares estimation algorithms[14, 20] implicitly locate discontinuities by minimizing the squared differences between unwrapped and wrapped gradients. Other approaches, like Goldstein's residue-cut algorithm [16] and Costantini's minimum cost flow algorithm [6] both use "path following" strategies that explicitly identify and place discontinuities.

If we define $\phi(i,j)$ and $\psi(i,j)$ as the unwrapped and the wrapped phase fields respectively, where the indices i,j live in a rectangular $M \times N$ grid, the measured phase will obey

$$\psi(i,j) = \mathcal{W}(\phi(i,j)) = \phi(i,j) + 2\pi n(i,j) \tag{1}$$

where $n(i,j)$ are integers such that $-\pi \leq \psi(i,j) < \pi$ and $\mathcal{W}$ is the wrapping operator.

Following Costantini[6], we define the residuals

$$k_q = k_{i,j,d} = \frac{1}{2\pi}[\Delta_d \phi(i,j) - \mathcal{W}(\Delta_d \psi(i,j))] \tag{2}$$

for each individual arc $q = \{i,j,d\}$, where Δ_d is the discrete difference operator along the direction $d \in \{x,y\}$. If we let $\psi_q = \psi_{i,j,d} = \mathcal{W}(\Delta_d \psi(i,j))$, then phase unwrapping can be formulated as

$$\min \sum_q c_q |k_q| \tag{3}$$

subject to the constraints that all loop integrals (e.g., see Figure 2) be zero:

$$k_a + k_b - k_c - k_d = -\frac{1}{2\pi}[\psi_a + \psi_b - \psi_c - \psi_d], \tag{4}$$

and where the $c_q \geq 0$ in (3) weight the confidence in the residuals. By rewriting (3),(4) in terms of

$$x_q^+ = \max(0, k_q), \quad x_q^- = \max(0, -k_q) \tag{5}$$

where $x_q^+ \geq 0, x_q^- \geq 0$, the nonlinear minimization problem can be converted into a linear minimum cost flow in a network for which efficient solutions exist, and for which the solutions are guaranteed to be integer [1, 6]. The following network structure was recognized by [6]:

- Each node represents one 2×2 loop integral (right hand side of (4)).
- Each node will be connected to each of four neighbors by two arcs, one for x_q^+ and one for x_q^-. The flow on each arc physically represents the residual (2).
- The costs c_q can be any positive function.

With the network defined, there are two inputs to the minimum cost flow solvers: The map of loop phase integrals, which are fixed by (4) for a given dataset, and the costs $c_q^\pm$ corresponding to flows $x_q^\pm$, which are the only free parameters to be chosen.

Figure 3 illustrates the influence of the costs. The network flow algorithm will connect the two opposite charges, since the constraints specify that all unbalanced charges must be neutralized. If the optimization is carried out with constant costs, the result will clearly be a straight line connecting the two charges. However under a modified cost function (Figure 3(b)) the new minimum-cost path will change (due to the symmetry of the problem there is a second optimal path, not shown, proceeding along the lower arc). Clearly the flow costs affect the optimal path connecting the charges; therefore the issue of cost selection must be of significance in phase unwrapping.

Different cost functions have evolved since unweighted network-flow[5]. Costantini[6] used the coherence map as weights; Ghiglia and Pritt[13] used Flynn's algorithm [9] with costs obtained by thresholding the phase slope variance map; Eineder *et al*[8] produced a binary cost map by thresholding the three variables of amplitude, charge density and flatness; Chen and Zebker[4] separately thresholded the coherence map and edge detection applied to the interferogram magnitude; finally in [21] a neural network was used. Although some of these studies have been very thorough, none of them have a supporting theory regarding the limitations or extensibility of the method.

3 Phase Aliasing Probabilities

The costs in (3) should be selected to guide the flow along paths where a terrain discontinuity is most likely, and therefore each weight needs to reflect somehow the probability of a residual. We begin our analysis by investigating the probability that a phase-gradient is aliased; that is, the probability that a residual will be required between two pixels:

$$\Pr\left\{\frac{1}{2\pi}[\Delta_d\phi(i,j) - \mathcal{W}(\Delta_d\psi(i,j))] \neq 0\right\}. \tag{6}$$

Our derivation of network-flow costs in Section 4 will be based on estimating these probabilities. We begin with a simple case in which the problem parameters are assumed to be error-free; we then refine the aliasing probabilities by incorporating uncertainties in the parameters themselves.

3.1 Phase Gradient PDF

Based on circular Gaussian statistics, [17] derived the probability density function for single-look and multi-look interferometric (unwrapped) phase distributions:

$$P_\phi(\phi|\gamma,\phi_T) = \frac{\Gamma(n+\frac{1}{2})(1-\gamma^2)^n\beta}{2\sqrt{\pi}\Gamma(n)(1-\beta^2)^{n+1/2}} + \frac{(1-\gamma^2)^n}{2\pi}F(n,1;\frac{1}{2};\beta^2), \tag{7}$$

where n is the number of looks, γ is the coherence (the magnitude of the complex correlation coefficient between the two SAR signals), $\beta = \gamma\cos(\phi-\phi_T)$, ϕ_T is the location of the peak of the distribution, Γ is the Gamma function, and F is the Gaussian hypergeometric function.

From Bamler[2], the decorrelation noise ϕ_N causes the wrapped interferogram $\phi = \phi_T + \phi_N$ to be a random process which deviates from the ideal topography ϕ_T. Since the noise component must satisfy $|\phi_N| < \pi$, it makes sense to truncate P_ϕ at the $\pm\pi$ interval centered on ϕ_T (as in Figure 4(a)).

Consider the PDF of the horizontal phase gradient δ_ϕ between nodes (i,j) and $(i+1,j)$; the corresponding PDF on arc $q = \{i,j,d=x\}$ is given by the convolution

$$P_q(\delta_\phi|\vec{X_q}) = P_\phi(\delta_\phi|\gamma(i+1,j),\phi(i+1,j)) * P_\phi(\delta_\phi|\gamma(i,j),-\phi(i,j)) \tag{8}$$

where γ is the pixel coherence, $\alpha = \phi_T(i+1,j) - \phi_T(i,j)$ is the topographic gradient, and $\vec{X_q} = [\alpha,\gamma(i+1,j),\gamma(i,j)]$ the vector of parameters corresponding to arc q. It is then straightforward to compute the desired residual probabilities:

$$p_q^{(-1)} = \int_{\alpha-2\pi}^{-\pi} P_q(\delta_\phi|\vec{X_q})d\delta_\phi\ ;\ \ p_q^{(0)} = \int_{-\pi}^{\pi} P_q(\delta_\phi|\vec{X_q})d\delta_\phi\ ;\ \ p_q^{(+1)} = \int_{\pi}^{\alpha+2\pi} P_q(\delta_\phi|\vec{X_q})d\delta_\phi. \tag{9}$$

Figure 4 shows the convolved PDF with the integration limits represented graphically. Note that except in the presence of very steep slopes, $p_q^{(r)} \approx 0$ for $|r| \geq 2$.

3.2 Parameter Inaccuracies

The derivation of the previous subsection is illustrative but incomplete, in the sense that the PDFs of each pixel involved in the convolution (8) depend on two parameters: the phase gradient α and the coherence γ. These parameters are *estimated* from the data and are subject to errors. In particular, a lower coherence leads to increased estimation error variances of both parameters[23, 24]. For example, a very low coherence over flat topography can lead to grossly inaccurate estimates of the gradient; if this gradient estimate $\hat{\alpha}$ is believed, then the inferred PDF will be highly skewed (as in Figure 4) predicting $p_q^{(+1)} \gg p_q^{(-1)}$, even though $p_q^{(+1)} \approx p_q^{(-1)}$ would have been more appropriate.

Instead, in principle we need to consider the joint PDF of the phase, gradient, and coherence. For the sake of simplicity, and because the influence of slope variability is much higher than that of coherence, we will assume that the coherence estimation is exact. We base this assumption on the observation that the distribution of the estimated slope is uniform as $\gamma \to 0$, an effect which does not occur for coherence. Empirically, we found that including coherence variation does not produce a significant altering of the results.

We begin with the equation for the probability of a zero residual

$$p_q^{(0)}(\hat{\alpha}, \hat{\gamma}) \quad = \quad \int_{-\pi}^{\pi} P_{\delta_\phi}(\delta_\phi | \hat{\alpha}, \hat{\gamma}) \; d\delta_\phi \tag{10}$$

where $\hat{\alpha}, \hat{\gamma}$ represent estimates. This distribution, $P_{\delta_\phi}()$, conditioned on the (possibly inaccurate) estimates

is not known, so we incorporate the dependence on the true underlying variables and find the marginal distribution:

$$p_q^{(0)}(\hat{\alpha},\hat{\gamma}) \;=\; \int_{-\pi}^{\pi} P_{\delta_\phi}(\delta_\phi|\hat{\alpha},\hat{\gamma})\; d\alpha\; d\delta_\phi = \int_{-\pi}^{\pi}\int\int P_{\delta_\phi}(\delta_\phi,\alpha,\gamma|\hat{\alpha},\hat{\gamma})\; d\alpha\; d\gamma\; d\delta_\phi. \tag{11}$$

We have argued that the error in the coherence is minor, compared to errors introduced by the slope estimation, so $\hat{\gamma} \simeq \gamma$ and we can write

$$p_q^{(0)}(\hat{\alpha},\hat{\gamma}) \;=\; \int_{-\pi}^{\pi}\int P_{\delta_\phi}(\delta_\phi,\alpha|\hat{\alpha},\hat{\gamma})\; d\alpha\; d\delta_\phi = \int_{-\pi}^{\pi}\int P_{\delta_\phi}(\delta_\phi|\alpha,\hat{\alpha},\hat{\gamma}) P_\alpha(\alpha|\hat{\alpha},\hat{\gamma})\; d\alpha\; d\delta_\phi \tag{12}$$

The former distribution is given by (8); the latter represents the distribution for the true slope, given the slope estimate. Since the prior model $P_\alpha(\alpha)$ for the slope will be entirely terrain dependent, we will choose a uniform distribution for the slope, which corresponds to a "maximum entropy" or least-information condition, in which case

$$P_\alpha(\alpha|\hat{\alpha},\hat{\gamma}) \;=\; P_{\hat{\alpha}}(\hat{\alpha}|\alpha,\hat{\gamma}) \tag{13}$$

and so the desired residual probability reduces to

$$p_q^{(0)}(\hat{\alpha},\hat{\gamma}) \;=\; \int_{-\pi}^{\pi}\int_{-\infty}^{\infty} P_q(\delta_\phi|\alpha,\hat{\gamma})\; P_\alpha(\hat{\alpha}-\alpha|\hat{\gamma})\; d\alpha\; d\delta_\phi \tag{14}$$

where $P_\alpha()$ represents the distribution of the estimated slope $\hat{\alpha}$ about the true value α.

Note that all of the phase distributions are defined over $[-\infty,\infty]$. The measured phase is wrapped, and so has a non-zero probability only over a limited range. The surface slope can only be estimated for slopes in the range $[-\pi,\pi]$, however in principle the surface slope α can have any value, and so is defined and

integrated over $[-\infty, \infty]$. The *measured* phase difference is limited to a range of $[-2\pi, 2\pi]$, however the *unaliased* phase difference is unlimited, so Figure 4 extends over $[-\infty, \infty]$.

It is clear that $p_q^{(0)}(\hat{\alpha}, \hat{\gamma})$ will depend on the particular method that has been chosen to compute the estimates. Both slope estimation[7, 23] and coherence estimation[10, 22, 24] have been active areas of research; *any* published algorithm could be used here, as long as the associated estimation error PDF required in (14), is known. Of course, better estimators will correspond to narrower estimation error PDFs, leading to more specific network-flow costs and better results.

For the examples shown in Section 5, we will estimate the slope using a Maximum Likelihood method [23]. The error statistics can be approximated as Gaussian, with a variance of [23]

$$\sigma_e{}^2 \approx p_o \pi^2/3 + (1 - p_o)\frac{6}{\gamma N(N-1)}, \qquad p_o = \frac{1}{N}\sum_{n=2}^{N} \frac{N!(-1)^n}{(N-n)!n!} \exp(-N\gamma \frac{n-1}{n}) \tag{15}$$

where N is the number of pixels of the square estimation window and γ is the coherence.

4 Maximum Likelihood Costs

Section 3 derived the probability of having aliased phase gradients; in this section we will proceed to exploit that information in order to derive an improved network-flow cost function. We begin by deriving the costs by analogy to a simple Maximum Likelihood problem, and then proceed to discuss some of the assumptions implicit in the analogy. It is important to keep in mind that this derivation is *not* an attempt to solve network flow analytically, rather the strategy is to arrive at a *similar*, simpler problem which yields some insights and theoretical expressions for the costs.

Suppose we have a phase unwrapping problem: the arc q between a pair of adjacent pixels has associated with it the discrete probability distribution of its residual k_q,

$$p_q^{(r)} = Pr(k_q = r | \vec{X}_q) \tag{16}$$

as derived in Section 3, where $\vec{X}_q$ is the vector of parameters (e.g., estimated slope, coherence) associated with the arc, defined in (8). Let us consider a random particular solution $\mathbf{k} = \{k_q\}$, over the space of all feasible solutions $\mathcal{K}$. Under the assumption that all of the residuals $\{k_q\}$ are independent, the probability of this ensemble is

$$Pr(\mathbf{k}) = \prod_r \prod_{k_q=r} p_q^{(r)} = \prod_q p_q^{(0)} \prod_{r\neq 0} \prod_{k_q=r} \frac{p_q^{(r)}}{p_q^{(0)}} \tag{17}$$

The Maximum Likelihood solution for $\mathbf{k}$ is given by the most probable assignment:

$$\begin{aligned}
\hat{\mathbf{k}} &= \arg\max_{\mathbf{k}} \mathcal{P}(\mathbf{k}) = \arg\max \prod_q p_q^{(0)} \prod_{r\neq 0} \prod_{k_q=r} \frac{p_q^{(r)}}{p_q^{(0)}} && (18)\\
&= \arg\max_{\mathbf{k}} \prod_{r\neq 0} \prod_{k_q=r} \frac{p_q^{(r)}}{p_q^{(0)}} && (19)\\
&= \arg\max_{\mathbf{k}} \sum_{r\neq 0} \sum_{k_q=r} \ln \frac{p_q^{(r)}}{p_q^{(0)}} && (20)\\
&= \arg\min_{\mathbf{k}} \sum_q \sum_{r\neq 0} \delta(k_q = r) \left(-\ln \frac{p_q^{(r)}}{p_q^{(0)}} \right) && (21)
\end{aligned}$$

where [arg] returns the value of $\mathbf{k}$ which optimizes the associated criterion. From (9) and the subsequent discussion we limit our consideration to $k_q \in \{-1, 0, +1\}$, in which case (21) becomes

$$\hat{\mathbf{k}} = \arg\min_{\mathbf{k}} \sum_q \left\{ \delta(k_q + 1) \left(-\ln \frac{p_q^{(-1)}}{p_q^{(0)}} \right) + \delta(k_q - 1) \left(-\ln \frac{p_q^{(+1)}}{p_q^{(0)}} \right) \right\} \tag{22}$$

However, out of the feasible set $\mathcal{K}$ network flow optimizes

$$\arg_{\mathbf{k}} \min \sum_q c_q^- x_q^- + c_q^+ x_q^+ . \tag{23}$$

Most network-flow implementations implicitly adopt $c_q^- = c_q^+$, however this limitation is not necessary. If we assume that $|x_q^\pm| < 2$, which will be true for almost all pixels, then the network-flow and maximum-likelihood objectives are equivalent if we equate terms in (22) and (23):

$$c_q^+ = -\ln \frac{p_q^{(+1)}}{p_q^{(0)}} \qquad c_q^- = -\ln \frac{p_q^{(-1)}}{p_q^{(0)}} \tag{24}$$

These cost expressions are the fundamental result of this paper.

Our derivation *does* assume that the residuals are independently distributed. This hypothesis is, of course, not completely valid, however the *a priori* correlation is weak.

We are interested in computing the *a priori* probability of having a residual r at a given arc q of the network, i.e., we would like to explore all possible paths that connect every combination of residues, without setting any preference or favoring one path over others.

For the sake of clarity, let us consider only two residues that need to be connected, R^+ and R^-. Any feasible solution must start at one of them, say R^+, and finish at R^-; that is the meaning of the constraint $k \in K$. Now if we consider all feasible paths, given an arbitrary arc q, the probability that q belongs to a selected path, only by virtue of existing in the network but without any further preference, will be related to the distance to any of those residues R^+ or R^-. The residual probability on any one of the four arcs coming out of R^+ will be 1/4; if we consider the next neighboring arcs their probability will be (1/4)(1/3) etc. That is, roughly speaking the probability evolves as a random walk, decreasing exponentially with distance.

Finally, an implicit assumption in our derivation is that zero-residuals must be the most probable; i.e., that $p_q^{(0)} \geq p_q^{(r)}$, otherwise the costs would become negative. From Figure 4, it should be clear that this is possible only for anomalously large estimates of the surface slope. If the estimated slope is bounded by $\pm\pi$, then cost positivity is guaranteed.

5 Results

This section presents four tests: the first based on an artificial toy problem, the next two based on standard benchmark unwrapping problems from the literature[13], and finally one ERS-Tandem [11] data set over Europe.

5.1 Implementation

The ML cost function (24) is straightforward to compute given the residual probabilities; the numerical complexity resides in evaluating the integrals (8), (9), (14). The required parameters are the estimated slope $\hat{\alpha}$ and the coherence values γ_1, γ_2 of neighboring pixels. The computational complexity can be reduced by using $\hat{\gamma} = \min(\gamma_1, \gamma_2)$, and by pre-constructing several 2-D look-up tables, shown in Figure 5, over the restricted ranges $-\pi \leq \alpha \leq \pi$ and $0 \leq \gamma \leq 1$.

We have used the RELAX-IV minimum cost flow algorithm by Bertsekas and Tseng [3].

5.2 Toy Problem

The "horseshoe" example of Figure 1 can be viewed as a rough caricature of an elevation peak projected to slant range. Of the many toy examples tested, this one is the most effective in illustrating the inability of the constant-costs approach to correctly unwrap.

Two parameters were varied: the width of the gap and the minimum coherence value. Figure 6 shows sample results for a coherence of 0.4, and for an average gap size. The constant cost function introduces long cuts that generate artificial discontinuities, whereas the ML costs guide all residuals along the low coherence area, producing the correct surface.

Table 1 summarizes the results of various tests. The errors are on the order of 20% for both alternatives when the gap width is very small. Opening the gap a little ($\geq$ 30 pixels) creates a high-coherence narrow band that allows the algorithm to correctly unwrap (4-5% error) in most combinations for the ML-costs case, whereas errors were systematically high with constant costs.

We should note that near the apex of the horseshoe the hypothesis from Section 4 that $|r| \leq 1$ is violated. As a consequence, at this point the network-flow result will deviate from the theoretical solution of the ML cost model. Specifically, network-flow will adopt cost $-|r| \cdot \ln(p_q^{(1)}/p_q^{(0)})$ rather than the cost $-\ln(p_q^{(r)}/p_q^{(0)})$ of maximum likelihood. In practice there are few such points in an image, so the distinction is relatively minor.

Note that setting costs by thresholding the coherence map would not necessarily solve this problem. An image containing multiple such horseshoes, at varying coherence contrasts, could not be successfully unwrapped on the basis of a single, global coherence threshold.

5.3 Synthetic SAR Data

A second test was performed on two synthetic data sets, which have been thoroughly tested by several phase unwrapping algorithms [13]. Figure 7 contains two sets of seven panels, including intensity-coded differences between the original surface and unwrapped results for three different unwrapping algorithms.

Our proposed approach yields excellent unwrapped surfaces with only local, individual-pixel errors, whereas network-flow with constant costs suffers from substantial errors of broad geographic extent.

Even compared with two of the most recent algorithms described in Ghiglia & Pritt [13], Flynn's in panel (f) and the minimum L^p-norm in (g), our algorithm performs at least as well: in both examples the only errors generated by these reference methods and our proposed approach are located at layover/foreshortening areas and at the boundaries of the external mask. All three algorithms are fully automatic: the costs are computed based on the data, and there are no parameters to tune in order to produce these results. The results are similar for all three methods: in terms of the total pixels incorrectly unwrapped, our proposed costs unwrap all but 3.85% of the pixels correctly, whereas the other two methods have unwrapping errors of 4.0% and 4.1%.

5.4 Etna Interferogram

One final example tests our algorithm on real data, a 512×512 pixel interferogram, taken from an ERS-1/2 Tandem dataset over Mt. Etna, Sicily, Italy. The test results are shown in Figure 8. In this example the coherence is high, but there are some severe deformations due to the viewing geometry of the SAR, generating long topographic flows, particularly near the peak of the volcano close to the center of the image. No unexpected effects can be observed in the surface unwrapped with the ML costs.

Unfortunately no reference elevation model was available, therefore we can only show the differences between our results and the two reference algorithms: Flynn and minimum L^p-norm.

6 Conclusions

The minimum cost flow algorithm is an effective tool for high quality unwrapping of interferograms. We have illustrated the dependence of the unwrapping path on the flow costs, motivating a new look at assessing these costs.

The costs required for the optimization have been derived theoretically by analogy with a maximum likelihood approach, which provides both an approximate model of the residual probabilities, and a practical algorithm for computing them. The resulting unwrapped interferograms are competitive with recently published algorithms.

One limitation of the proposed method is the assumption of residual independence; further work is required to refine the probabilistic models, specifically taking into account correlations due to the data and those induced by the flow constraints.

Our contribution is an *approach* to assigning costs, rather than a specific algorithm. Because our approach is based on statistical models of slope and coherence estimates, our method can *already* accommodate future developments, such as improved slope and coherence estimators or statistical terrain height information provided by approximate digital elevation models.

References

[1] R. Ahuja, T. Magnanti, J. Orlin, *Network Flows: Theory, Algorithms, and Applications*. Englewood Cliffs: Prentice-Hall, 1993.

[2] R. Bamler, N. Adam, G. Davidson, D. Just, "Noise-induced slope distorsion in 2-D phase unwrapping by linear estimators with application to SAR Interferometry ", *IEEE Trans. Geosci. Remote Sens.*, vol. 36, pp. 913-921, 1998.

[3] D. Bertsekas, P. Tseng, "The relax codes for linear minimum cost network flow problems", *Annals of Operations Research*, vol. 13, 1988.

[4] C. Chen, H. Zebker, "Network approaches to two-dimensional phase unwrapping: intractability and two new algorithms ", *submitted to IEEE Trans. Geosci. Remote Sens.*

[5] M. Costantini, "A phase unwrapping method based on network programming", in *Proc. Fringe '96 Workshop ERS SAR Interferometry*, Zurich, Switzerland, ESA SP-406, pp. 261-272, 1996.

[6] M. Costantini, "A novel phase unwrapping method based on Network Programming", *IEEE Trans. Geosci. Remote Sens.*, vol. 36, pp. 813-821, 1998.

[7] G. Davidson, R. Bamler, "Multiresolution phase unwrapping for SAR Interferometry ",*IEEE Trans. Geosci. Remote Sens.*, vol. 37, pp. 163-174, 1999.

[8] M. Eineder, M. Hubig, B. Milcke, "Unwrapping large interferograms using the minimum cost flow algorithm ", in *Proc. IGARSS '98*, Seattle, WA, pp. 83-87, 1998.

[9] T. Flynn, "Two-dimensional phase unwrapping with minimum weighted discontinuity", *J. Opt. Soc. Am. A*, vol. 14, pp. 2692-2701, 1997.

[10] M. Foster, J. Guinzy, “The coefficient of coherence: its estimation and use in geophysical data processing”, *Geophysics*, vol. 23, pp. 602-616, 1967.

[11] D. Furseth, A. Ray, K. Jones, “RADARSAT repeat-pass interferometry - operational issues, opportunities, and planning tools”, in *Proc. IGARSS ’99*, Hamburg, Germany, 1999.

[12] R. Gens, J. Van Genderen, “SAR Interferometry - issues, techniques, applications”, *Int. J. Remote Sensing*, vol. 17, pp. 1803-1835, 1996.

[13] D. Ghiglia, M. Pritt, *Two-Dimensional Phase Unwrapping: Theory, Algorithms, and Software*, New York, NY: Wiley, 1998.

[14] D. Ghiglia, L. Romero, “Robust two-dimesional weighted and unweighted phase unwrapping that uses fast transforms and iterative methods”, *J. Opt. Soc. Am. A*, vol. 11, pp. 107-117, 1994.

[15] D. Ghiglia, L. Romero, “Minimum L^p-norm two-dimensional phase unwrapping”, *J. Opt. Soc. Am. A*, vol. 13, pp. 1999-2013, 1996.

[16] R. Goldstein, H. Zebker, C. Werner, “Satellite radar interferometry: two-dimensional phase unwrapping”, *Radio Sci.*, vol. 23, pp. 713-720, 1988.

[17] J.S. Lee et al., “Intensity and phase statistics of multilook polarimetric and interferometric imagery”, *IEEE Trans. Geosci. Remote Sens.*, vol. 32, Sept. 1995.

[18] O. Loffeld, R. Krämer, “Phase unwrapping for SAR Interferometry”, in *Proc. IGARSS ’94*, pp. 2282-2284, 1994.

[19] C. Prati, F. Rocca, A. Monti Guarnieri, P. Pasquali, “ERS-1 SAR interferometric techniques and applications”, ESA Contract Report - ESRIN Contract N. 3-7439/92/HGE-I.

[20] M. Pritt, “Phase unwrapping by means of multigrid techniques for interferometric SAR”, *IEEE Trans. Geosci. Remote Sens.*, vol. 34, pp. 728-738, 1996.

[21] A. Refice, G. Satalino, S. Stramaglia, M. Chiaradia, N. Veneziani “Weights determination for minimum cost flow InSAR phase unwrapping”, in *Proc. IGARSS ’99*, Hamburg, Germany, 1999.

[22] M. Seymour, I. Cumming, “Maximum Likelihood estimation for SAR Interferometry”, in *Proc. IGARSS ’94*, pp. 2282-2285, 1994.

[23] U. Spagnolini, “2-D phase unwrapping and instantaneous frequency estimation”, *IEEE Trans. Geosci. Remote Sens.*, vol. 33, pp. 579-589, 1995.

[24] R. Touzi, A. Lopes, J. Bruniquel, P. Vachon, “Coherence estimation for SAR Imagery”, *IEEE Trans. Geosci. Remote Sens.*, vol. 37, pp. 135-149, 1999.

[25] H. Zebker, R. Goldstein, “Topographic mapping from interferometric SAR observations”, *J. Geophysical Res.*, vol. 91, pp. 4993-4999, 1986.

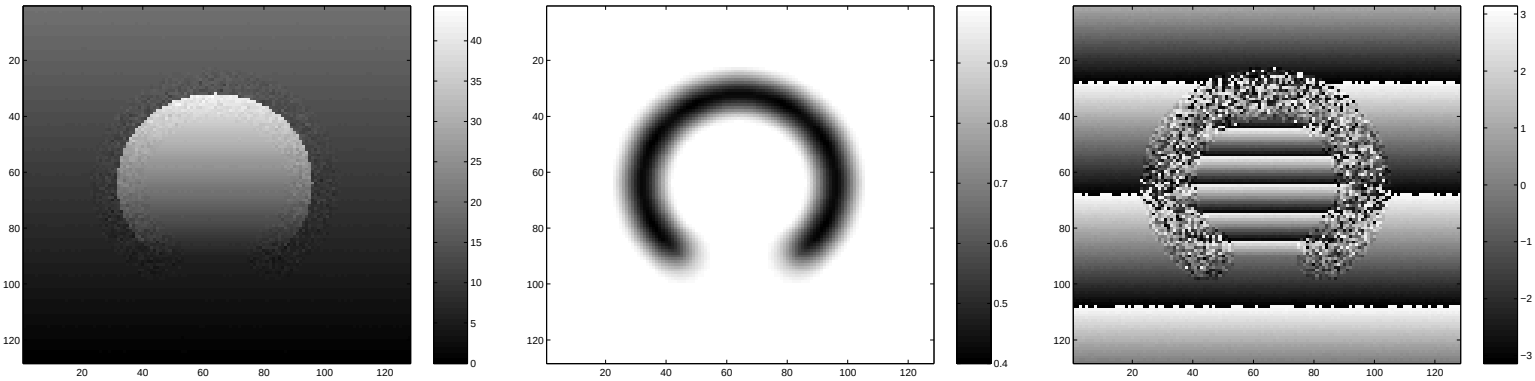

(a) (b) (c)

Figure 1:

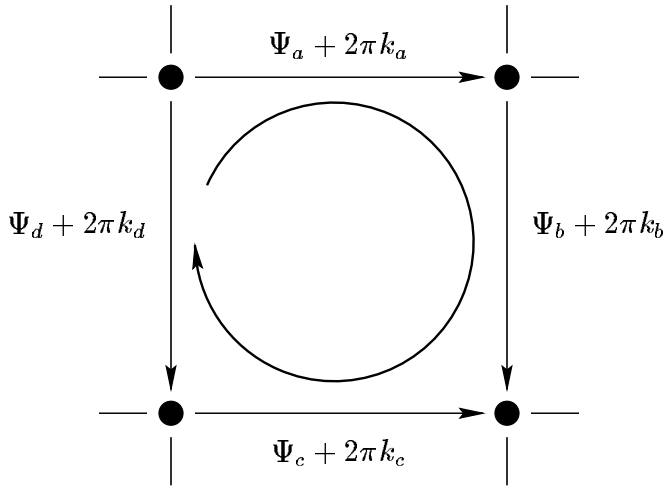

Figure 2:

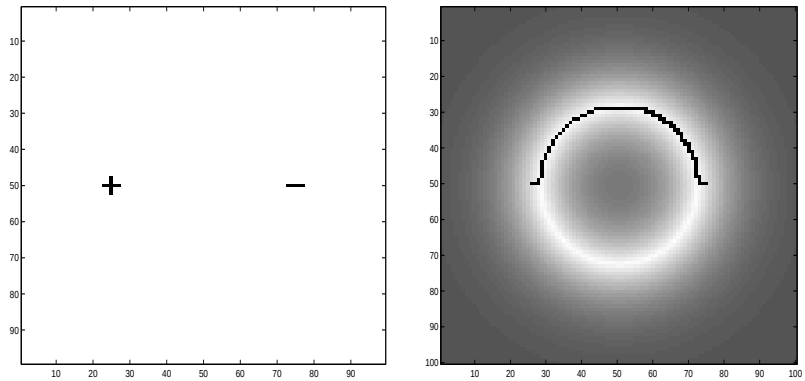

(a) (b)

Figure 3:

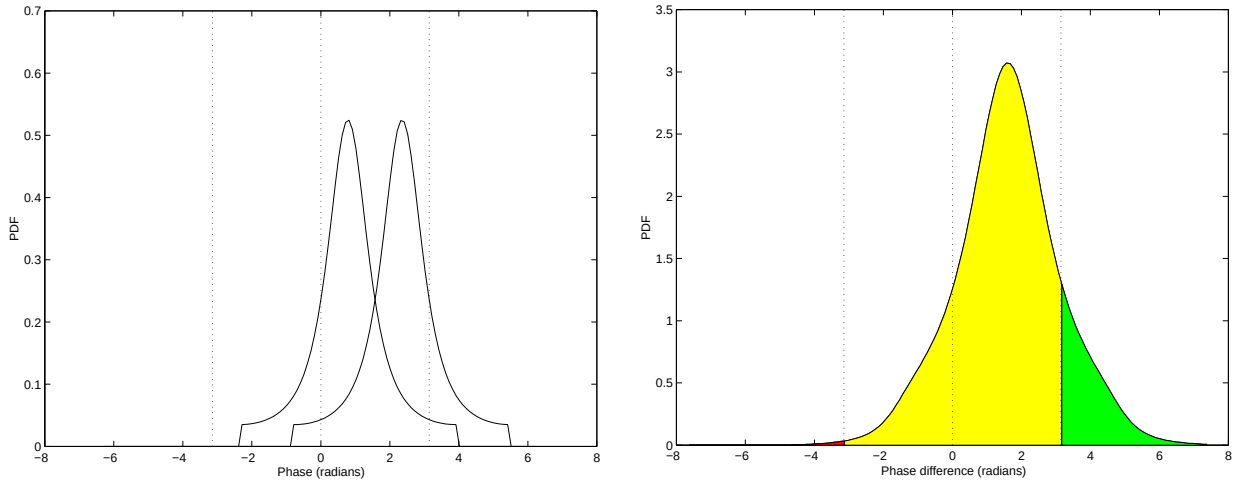

(a) (b)

Figure 4:

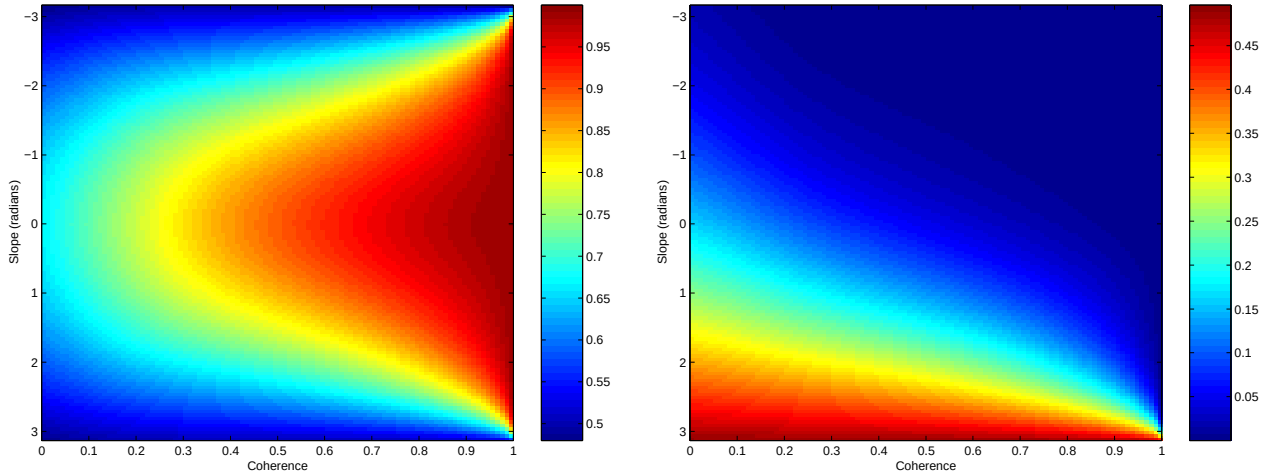

(a) (b)

Figure 5:

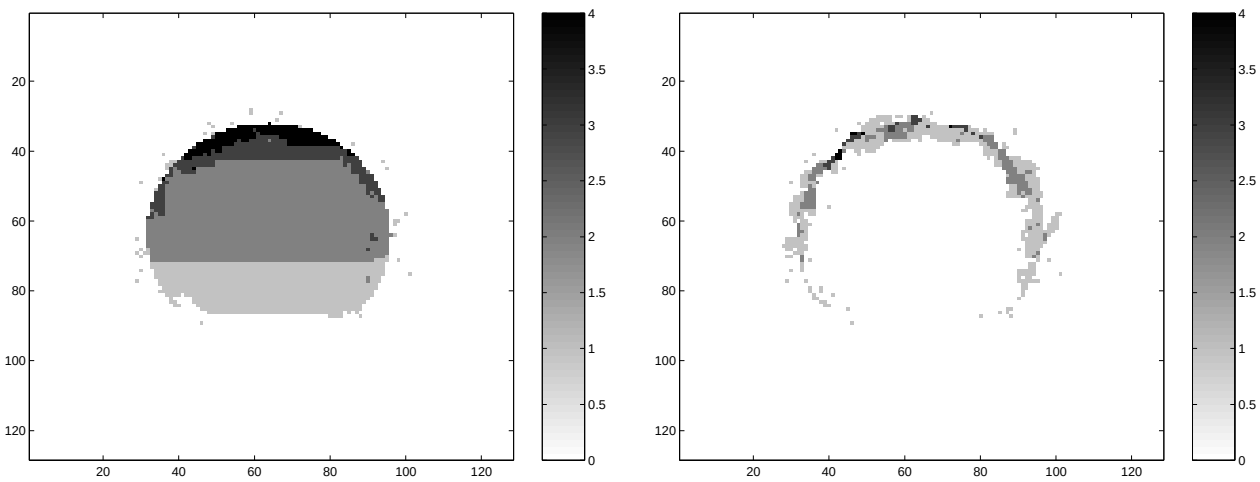

(a) (b)

Figure 6:

Test #	Minimum Coherence	Gap Width (Pixels)	% Pixels in Error (Constant Costs)	% Pixels in Error (ML Weighted Costs)
1	0.1	20	20.6	20.8
2	0.2	20	20.6	21.1
3	0.3	20	19.5	21.5
4	0.4	20	19.4	20.3
5	0.1	30	19.5	5.2
6	0.2	30	19.4	5.7
7	0.3	30	19.2	5.2
8	0.4	30	19.0	20.5
9	0.1	38	18.9	4.9
10	0.2	38	18.4	4.6
11	0.3	38	17.0	4.7
12	0.4	38	18.8	4.1
13	0.1	45	15.0	4.8
14	0.2	45	15.5	4.6
15	0.3	45	18.0	3.5
16	0.4	45	16.9	3.9

Table 1:

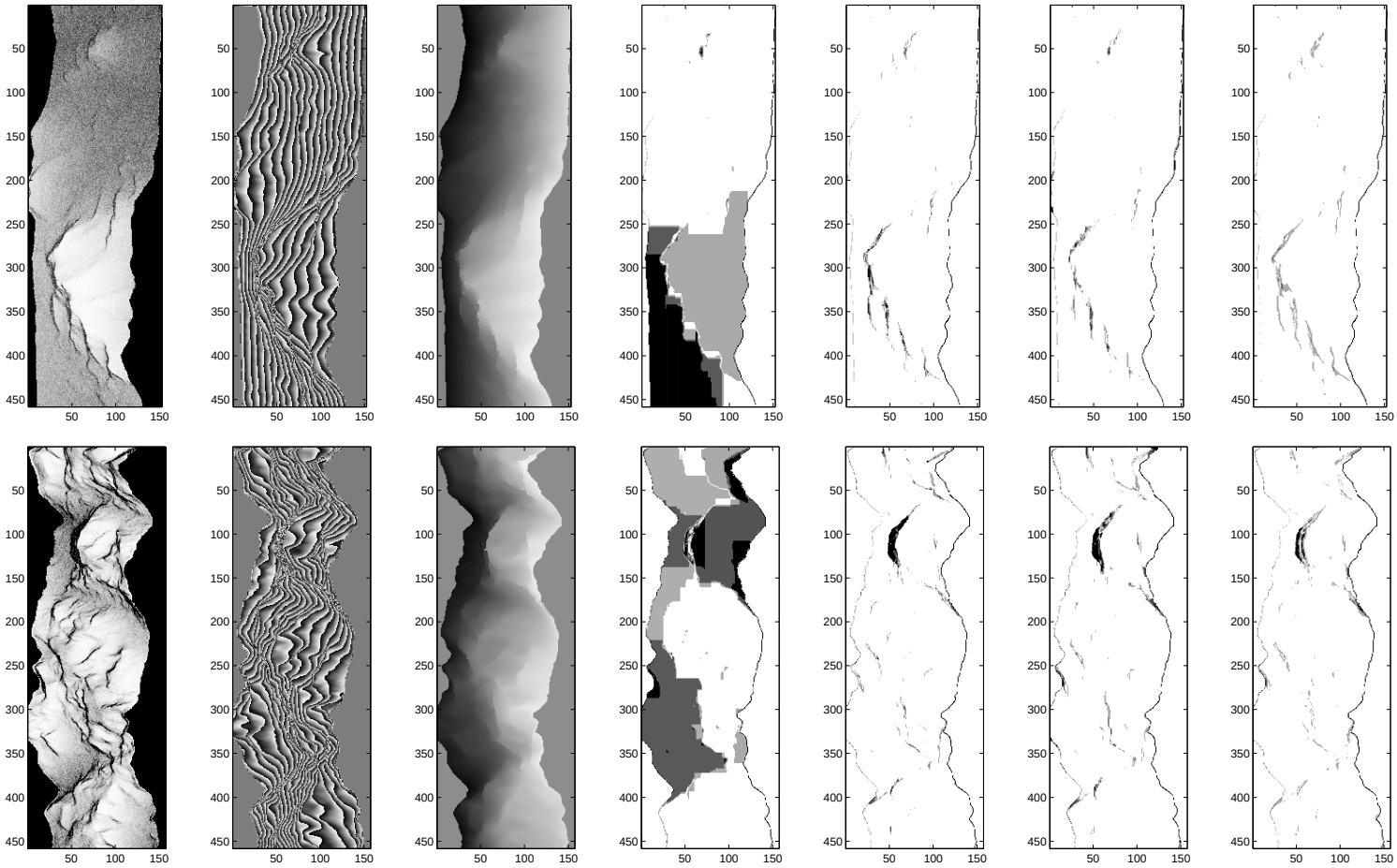

(a) (b) (c) (d) (e) (f) (g)

Figure 7:

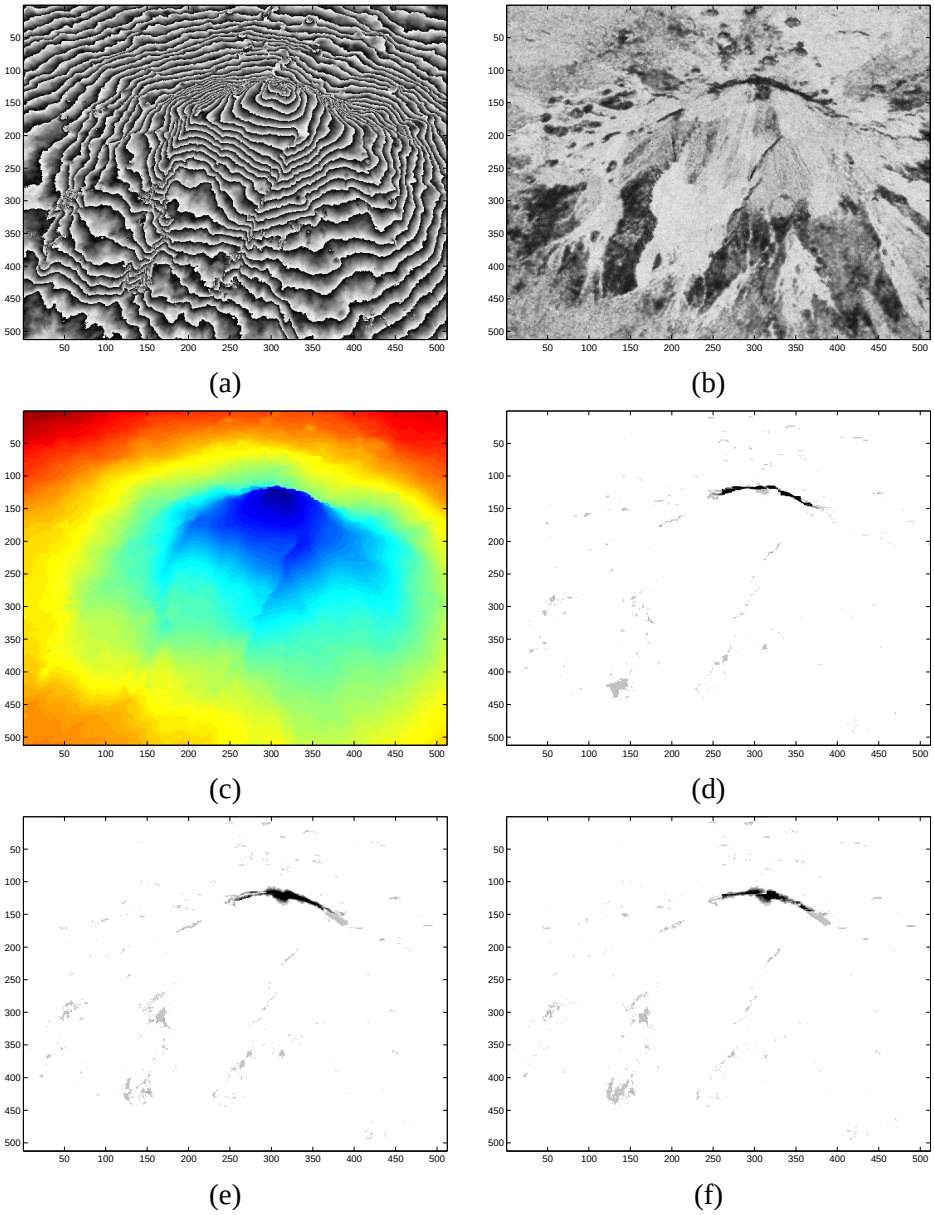

Figure 8:

Figure Captions

Figure 1: A simple, synthetic phase-unwrapping example. The 128×128 pixel surface (a) is composed of two ramps with different slopes; the pixel noise is Gaussian with single-look SAR variance[18] consistent with the coherence (b), which is low (0.4) near discontinuities in the surface and high (0.98) elsewhere. The wrapped phase (c) is computed from the noisy surface in (a).

Figure 2: A loop of four arcs; the integrated phase (4) about each such loop must equal zero.

Figure 3: (a) A sample charge map, composed of two opposite charges. (b) The resulting path produced by network flow, given a variable surface of costs (white represents lowest cost).

Figure 4: PDF's of two adjacent pixels, shown in (a). The peaks are located at $\pi/4$ and $3\pi/4$, and $\gamma = 0.7$. The vertical lines show the wrapping boundaries $\pm\pi$ and zero as a reference. Note how the PDFs exceed those boundaries. The PDF of the noisy phase difference obtained by convolving the two curves shown in (a), according to equation (8), is shown in (b). The shaded polygons represent the integrals in equation (9), from left to right $p_q^{(-1)}$, $p_q^{(0)}$ and $p_q^{(+1)}$.

Figure 5: Pre-computed 2-D look-up tables showing the probability distributions used to compute the costs using equation (24). This example corresponds to the single-look case and using a Maximum Likelihood estimator for the slope. The probability of a zero residual $p_q^{(0)}$ is shown in (a), the probability to be positive $p_q^{(+1)}$ is shown in (b). The look-up table for $p_q^{(-1)}$ is symmetric with (b), and can be found by reversing the vertical axis.

Figure 6: Differences between the unwrapped and the noisy "horseshoe" surface of Figure 1 for (a) constant costs, and (b) the proposed "Maximum Likelihood" costs. The minimum coherence is 0.4 and the gap is 38 pixels wide.

Table 1: Several tests were run in order to assess the "horseshoe" example of Figure 1. Two parameters are varied: the minimum coherence value at the discontinuity and the gap (measured in pixels) between the two endpoints of the discontinuity. The last two columns show the percentage of incorrectly unwrapped pixels, when measured against the original surface, for both constant and ML-varying costs.

Figure 7: Two synthetic examples taken from [13]. The coherence maps are shown in (a) (low coherence is black, high coherence is white). The interferograms are shown in (b), and the unwrapped phase fields obtained by our method are displayed in (c). The remaining panels show the *differences* between the original surface and four unwrapping algorithms: (d) constant-costs, (e) our proposed ML costs, (f) Flynn's method, (g) minimum L^p-norm. The latter two represent the best methods selected by Ghiglia & Pritt [13].

Figure 8: ERS-1/2 Tandem pair over Mount Etna, in Sicily, Italy; a 512×512 subset of the interferogram is shown in (a), the coherence in (b). The surface unwrapped using our costs is shown in (c). The difference between our ML costs result and those of Flynn's algorithm and the Minimum L^p-norm method are shown in (d), (e) respectively. Finally the difference between these two reference algorithms is depicted in (f).